

Mapping Jupiter's Mischief

Channon Visscher

¹Dordt University, Sioux Center, IA
²Space Science Institute, Boulder, CO

Key Points:

- Recent *Juno* results provide updated latitudinal abundance profiles that map the distribution of several key atmospheric species on Jupiter.
- Mapping key gases in Jupiter's troposphere characterizes the chemical and dynamical processes responsible for Jupiter's banded appearance.
- Chemistry in Jupiter's troposphere is tied to element abundances in the deep atmosphere, providing constraints for Jovian formation models.

Corresponding author: Channon Visscher, channon.visscher@dordt.edu

Abstract

New results (Grassi et al., 2020) from analysis of *Juno* Jovian Infrared Auroral Mapper (JIRAM) 4-5 μm observations provide updated latitudinal abundance profiles and measurements of the spatial distribution of H_2O , NH_3 , PH_3 , GeH_4 , and AsH_3 in Jupiter’s troposphere near the 3-5 bar level. The observed compositional variations provide new constraints on processes shaping chemical abundances in the cloud-forming region of the troposphere, including vertical and horizontal atmospheric mixing, meteorology and cloud formation, transport-induced quenching, and photochemistry. Along with recent results from the *Juno* Microwave Radiometer (MWR) for NH_3 and H_2O abundances far below the clouds, the JIRAM measurements of key disequilibrium tracer species can also be used to explore the coupled dynamics, chemistry, and bulk composition of Jupiter’s deep atmosphere. The heavy element abundance inventory on Jupiter is a key constraint for the development and assessment of giant planet formation models. Combined with prior ground-based, spacecraft, and *in-situ* observations, the *Juno* results suggest near-uniform ($\sim 2\text{-}4\times$) enhancements over protosolar abundances for several heavy elements in Jupiter’s atmosphere, giving new clues about the composition of the material accreted, the timing and location of formation, and the internal evolution of Jupiter over the history of the Solar System.

Plain Language Summary

New results from the *Juno* spacecraft provide high-resolution measurements of the distribution of several key gases in Jupiter’s atmosphere, and show how their abundances vary with latitude. The observed abundance distributions result from a complex tangle of chemical and physical processes, including atmospheric circulation, chemical reactions, and cloud formation that together shape the abundances of chemical species in the troposphere. Recent infrared and microwave measurements also provide key clues about the chemistry and composition of Jupiter’s atmosphere below the clouds and into the deep interior. The new results from the *Juno* mission thus represent a major step toward completing its goal of providing an accurate elemental inventory of Jupiter’s deep atmosphere, and deliver new insights into Jupiter’s formation and chemical evolution: what is Jupiter made of, and how did it get that way?

Prelude to *Juno*

Jupiter is the most massive planet in the Solar System, and played a central role in shaping the formation history, architecture, and composition of the planets. Important clues about early planetary history can thus be found in our understanding of Jupiter’s structure and chemical composition. For example, Jupiter consists mostly of hydrogen with a bulk composition roughly similar to that of the Sun, suggesting that Jupiter (and other H-rich giant planets) formed while there was still enough H and He gas in the protoplanetary disk available for significant accretion (for reviews, see Lunine et al., 2004; Taylor et al., 2004). Moreover, observations of exoplanetary systems showing evidence of planetary migration, along with modern dynamical models, suggest that Jupiter drove planetesimal migration and accretion throughout the early Solar System (e.g., see Gomes et al., 2005; Tsiganis et al., 2005; Helled et al., 2014; D’Angelo & Lissauer, 2018; Raymond et al., 2018, and references therein). Jupiter thus provides a record of the formation and earliest evolution of our own planetary system, and serves as a prototype for similar formation processes in exoplanetary systems.

Theoretical models and infrared observations also show that Jupiter emits nearly twice as much energy as it absorbs from the Sun, suggesting a hot, convective interior. For this reason, gas abundances in the troposphere of Jupiter have generally been considered (while accounting for cloud formation) indicative of its bulk composition. A key constraint for Jovian formation models is thus the comparison of model results to the



Figure 1. Jupiter near 56° N as seen by *Juno* from a distance of 15,500 km during its 13th perijove encounter. The bright clouds are inferred to be high clouds of NH_3 , with darker cloud material located deeper in the atmosphere. *Juno*Cam visible light image with colors exaggerated. Image credit: NASA/JPL-Caltech/SwRI/MSSS/Gerald Eichstädt/Seán Doran (CC NC SA).

62 observed abundances of compounds such as CH_4 , NH_3 , H_2S , and H_2O , etc., taken to rep-
 63 resent the planetary elemental abundances of the “heavy elements” C, N, S, and the ma-
 64 jority of planetary O, respectively. For example, *in-situ* measurements of Jupiter’s tro-
 65 posphere by the *Galileo* Probe Mass Spectrometer (GPMS; e.g., Mahaffy et al., 2000;
 66 Wong et al., 2004) showed enhancements in heavy-element-to- H_2 ratios for several el-
 67 ements (C, N, S, Ar, Kr, Xe) and depletions in others (e.g., Ne, O) relative to the orig-
 68 inal (or “protosolar”) element inventory of the Solar System. In this context, the suc-
 69 cess of planetary formation and evolution models are measured by their ability to repro-
 70 duce the observed enrichments and/or depletions. An accurate determination of Jupiter’s
 71 global element inventory has thus become a major goal of planetary research.

72 However, efforts to determine some representative Jovian composition have posed
 73 a challenging task. Jupiter is not a *tame* planet. High clouds of icy NH_3 or storm-driven
 74 H_2O clouds obscure deeper atmospheric levels (e.g., see Figure 1). And recent observa-
 75 tions suggest an atmosphere as variable and tumultuous as the swirling clouds suggest
 76 (e.g., de Pater et al., 2016; Bolton et al., 2017; Li et al., 2017; Fletcher, 2017; Antuñano
 77 et al., 2019; Fletcher et al., 2020). Although the *Galileo* Probe provided crucial measure-
 78 ments of Jupiter’s troposphere, it descended into an anomalously dry “hot spot” region
 79 (features found along the boundary between the equatorial zone and the north equator-
 80 ial belt) characterized by low cloud opacity, low abundances of cloud-forming species,
 81 high thermal ($5\ \mu\text{m}$) emission, and a water abundance that was still increasing with depth

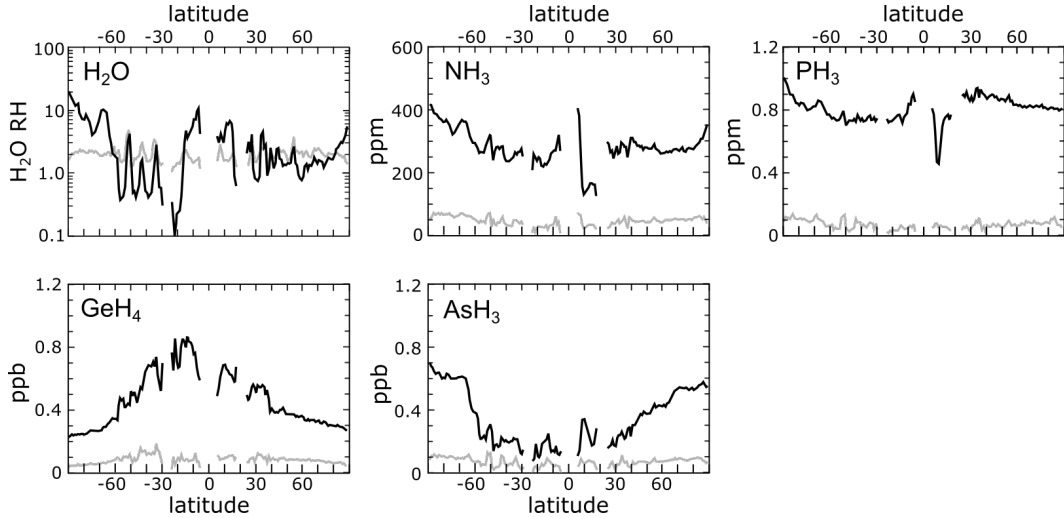


Figure 2. Averaged latitudinal profiles for H_2O (relative humidity), NH_3 , PH_3 , GeH_4 and AsH_3 (mole fractions) from Grassi et al. (2020) using *Juno* JIRAM observations from the first 15 perijove encounters (PJ1-PJ15). The black curves represent mean abundance values and the gray curves represent the standard deviation over all PJ1-PJ15 profiles. Gaps in the abundance profiles occur at latitudes with high aerosol opacity (corresponding with cloud-thick zones), where measurements of the gas composition are difficult to obtain. See Grassi et al. (2020) for details.

82 when the probe signal was lost at the 22-bar level (e.g., Wong et al., 2004; Orton et al.,
 83 1998; Niemann et al., 1998). So the question remained to what extent the GPMS results
 84 for H_2O could be taken as representative of some deep, well-mixed oxygen inventory for
 85 Jupiter as a whole. The *Juno* mission was designed to remotely sound the deep atmo-
 86 sphere to hundreds of bars, far beneath the upper veil of clouds, to address such global
 87 questions about Jupiter’s interior structure and bulk composition – and, in turn, its for-
 88 mation and chemical evolution.

89 *Juno* at Jupiter

90 Launched in the summer of 2011, *Juno* entered an eccentric polar orbit of Jupiter
 91 in the summer of 2016, swooping closely past the planet (less than 5000 km above the
 92 cloud tops) every 53.5 days. The major scientific products of these encounters are now
 93 coming to light. New results by Grassi et al. (2020) map the distribution of key atmo-
 94 spheric gases in Jupiter’s atmosphere using data collected by the Jovian Infrared Au-
 95 roral Mapper (JIRAM) over the first two years of *Juno*’s orbit (August 2016 to Septem-
 96 ber 2018). The JIRAM observations at 4-5 μm are sensitive to thermal emission from
 97 the cloud-formation region near $\sim 3\text{-}5$ bar (with clouds in silhouette against a bright back-
 98 ground), along with spectral features from several tropospheric gases. Grassi et al. (2020)
 99 performed retrieval analysis on a subset of available JIRAM data, using spectra selected
 100 for relatively high radiance, low emission angle, and high resolution. The *Juno* space-
 101 craft measurements provide two key advantages over previous observations: very high
 102 resolution (courtesy of its close proximity to Jupiter), and coverage at high latitudes us-
 103 ing similar viewing geometries as for low latitudes (courtesy of its polar orbit).

104 Grassi et al. (2020) provide new latitudinal abundance profiles (summarized in Fig-
 105 ure 2) and map the distribution of H_2O , NH_3 , PH_3 , GeH_4 , and AsH_3 in the cloud-forming
 106 region of Jupiter’s troposphere. The results also allow for new analysis of persistent cor-
 107 relations of gas abundances within discrete regions on Jupiter (e.g., belts and polar re-

gions), and – in the case of water vapor relative humidity – possible associations with zonal wind patterns (Grassi et al., 2020). The observed tropospheric abundances result from a tangle of closely coupled chemical, dynamical, and radiative processes, including vertical and horizontal mixing, meteorology and cloud formation, thermochemical kinetics and disequilibrium, and photochemistry. The *Juno* results thus provide new constraints for a range of models exploring how such processes conspire to shape the chemical composition of Jupiter’s troposphere. The new results also represent another major step toward completing *Juno*’s goal of mapping key species (including disequilibrium species) to provide an accurate elemental inventory of Jupiter’s deep atmosphere.

Chemical Connections to the Deep

A number of the minor species observed in Jupiter’s troposphere (including CO, PH₃, GeH₄, and AsH₃) are present in abundances that far exceed those expected from thermodynamic equilibrium. As was first demonstrated for CO (Prinn & Barshay, 1977), this behavior represents vertical mixing from deeper, denser, warmer levels where the species in question has a higher abundance at an equilibrium maintained by fast reaction kinetics (i.e., chemical timescales are short relative to mixing timescales, $\tau_{\text{chem}} < \tau_{\text{mix}}$). However, departures from equilibrium can occur at higher, cooler altitudes where convective vertical mixing occurs faster than chemical reactions can maintain equilibrium (i.e., $\tau_{\text{chem}} > \tau_{\text{mix}}$), effectively “quenching” the abundance of a molecular species at a fixed value throughout the upper troposphere. For most disequilibrium species, the “quench level” for this transition (i.e., $\tau_{\text{chem}} \approx \tau_{\text{mix}}$) is typically near 600–1000 K (Fegley & Prinn, 1985; Fegley & Lodders, 1994; Visscher & Moses, 2011; Wang et al., 2016). The observed tropospheric abundances of tracer species such as CO, PH₃, GeH₄, and AsH₃ thus provide a window to the dynamics, chemistry, and composition of Jupiter’s deep atmosphere down to \sim kilobar levels (e.g., Giles et al., 2017a; Grassi et al., 2020).

For example, PH₃ is expected to be the dominant P-bearing phase at high temperatures in Jupiter’s deep atmosphere, but is subject to removal by oxidation and/or condensation at lower temperatures (< 500 K). There has been some debate regarding the identity of the lower temperature P-bearing phase, mostly due differences in thermodynamic data adopted for phosphorus oxides such as P₄O₆ (for discussion, see Fegley & Lodders, 1994), and various compounds have been considered to replace PH₃ at lower temperatures, including: P₄O₆ (Fegley & Lodders, 1994; Visscher et al., 2006), P₄O₁₀ (Borunov et al., 1995), H₃PO₄ (Wang et al., 2016) and/or NH₄H₂PO₄ (Fegley & Lodders, 1994; Visscher et al., 2006; Morley et al., 2018). In any case, there is consensus that disequilibrium PH₃ observed in the troposphere comes from a deep atmospheric source representative of Jupiter’s elemental P inventory. However, the observed PH₃ abundance – possibly including the deep abundance – varies as a function of latitude in both 5 μm (e.g., Drossart et al., 1990; Giles et al., 2015, 2017a; Grassi et al., 2020) and mid-infrared (e.g., Irwin et al., 2004; Fletcher et al., 2009, 2016) observations. Notably, mid-infrared PH₃ values have typically been $\sim 2\times$ higher than the 5 μm values, and show an equatorial maximum as high as ~ 2 ppm PH₃ (e.g., see Fletcher et al., 2009, 2016) in the same location as the NH₃ maximum (de Pater et al., 2016; Li et al., 2017). Both PH₃ and NH₃ also show minima near 10°N in the JIRAM data (see Figure 2), suggestive of similar dynamical influences. Adopting the ~ 1 ppm PH₃ abundance maximum observed by JIRAM (near the south pole, see Figure 2; Grassi et al., 2020) as a lower limit for the deep PH₃ abundance yields a Jovian phosphorus inventory of at least $1.3\times$ the protosolar value.

Germane (GeH₄) is also subject to removal by condensation at temperatures below 700 K yet survives at \sim ppb disequilibrium concentrations into Jupiter’s upper troposphere. Because Ge is distributed among several Ge-bearing species at high-temperatures (Fegley & Lodders, 1994), GeH₄ cannot be taken as representative of Jupiter’s bulk Ge inventory (note that 1 ppb GeH₄ corresponds to $0.1\times$ the protosolar Ge abundance). Nevertheless, quenched GeH₄ is expected to show strong sensitivity to the convective mixing rate

160 compared to PH_3 or AsH_3 (Fegley & Prinn, 1985; Fegley & Lodders, 1994; Wang et al.,
 161 2016). Noting that convective mixing will be stronger at low latitudes on a rotating planet
 162 such as Jupiter (Flasar & Gierasch, 1977; Visscher et al., 2010), Wang et al. (2016) demon-
 163 strated that higher GeH_4 abundances would be expected near the equator than near the
 164 poles, in agreement with the latitudinal trends observed by JIRAM (e.g., see Figure 2
 165 and Grassi et al., 2020; Giles et al., 2017a, for discussion and comparison of observed trends).

166 On the other hand, the AsH_3 abundance is expected to be less sensitive to the rate
 167 of mixing (Fegley & Lodders, 1994; Wang et al., 2016) and the latitudinal profile of tropo-
 168 spheric AsH_3 is enigmatic, with an abundance that *increases* toward the poles (see
 169 Figure 2; Giles et al., 2017a; Grassi et al., 2020). Although the chemical scale height for
 170 each disequilibrium species differs depending upon reaction kinetics and quench condi-
 171 tions, each is presumably subject to the same convective transport. The unexpected AsH_3
 172 profile thus suggests that the chemical processes shaping the AsH_3 abundance remain
 173 incompletely understood. As suggested by Giles et al. (2017a), the observed distribu-
 174 tion is plausibly explained by photolytic destruction of AsH_3 in Jupiter’s upper tropo-
 175 sphere (analogous to NH_3 and PH_3 photochemistry near 200 mbar; Strobel, 1977; Kaye
 176 & Strobel, 1983), where higher photolysis rates toward the equator yield less AsH_3 . As-
 177 suming that AsH_3 is the dominant As-bearing in Jupiter’s deep atmosphere (Fegley &
 178 Lodders, 1994), the maximum AsH_3 abundance of 0.7 ppb measured by Grassi et al. (2020)
 179 suggests an enhancement of $\sim 1.3\times$ the protosolar value, similar to that observed for PH_3 .

180 Jupiter’s deep atmospheric water abundance (and more generally, Jupiter’s oxy-
 181 gen inventory) is critical to our understanding of Jupiter’s formation as well as dynam-
 182 ical and chemical processes (such as cloud formation) in Jupiter’s troposphere. Prior to
 183 *Juno*, however, the obscuring presence of clouds and other opacity sources have long lim-
 184 ited our ability to determine the H_2O abundance below the clouds. Earth-based infrared
 185 observations must contend with telluric H_2O contamination (e.g., see Bjoraker et al., 2016,
 186 2018) whereas centimeter measurements must account for synchrotron emission from Jupiter’s
 187 radiation belts (e.g., de Pater et al., 2016). Moreover, as noted above, it is unclear to
 188 what extent near-infrared observations (most sensitive to hot spot regions) or the GPMS
 189 measurement ($X_{\text{H}_2\text{O}} = 420 \pm 140$ ppm, corresponding to $\sim 0.5\times$ the protosolar $\text{H}_2\text{O}/\text{H}_2$
 190 ratio) can be taken as representative of the bulk planetary inventory.¹

191 Given these challenges, several investigators turned to chemical models to estimate
 192 the H_2O abundance by considering how water in the deep atmosphere influences the ob-
 193 served behavior of other species (in particular CO) mixed into the upper troposphere.
 194 For example, the ~ 1 ppb CO observed in Jupiter’s troposphere (e.g., Bézard et al., 2002;
 195 Bjoraker et al., 2018) is far greater (over 20 orders of magnitude) than the equilibrium
 196 abundance predicted near the 6-bar level, suggesting rapid vertical mixing from deeper
 197 in the atmosphere where CO is more abundant and forms via net reactions such as $\text{CH}_4 +$
 198 $\text{H}_2\text{O} \rightleftharpoons \text{CO} + 3\text{H}_2$. For a given carbon inventory (characterized by CH_4), the observed
 199 (quenched) abundance of CO thus depends upon the rate of reactions that interconvert
 200 $\text{CO} \rightleftharpoons \text{CH}_4$, the strength of convective vertical transport, and the abundance of water in
 201 the deep atmosphere: more H_2O yields more CO.

202 Following the approach pioneered by Prinn and Barshay (1977) and Fegley and Prinn
 203 (1988), modern numerical studies of H-C-O chemistry in Jupiter’s atmosphere use ex-
 204 tensive reaction networks to estimate the H_2O abundance based upon CO quench kinet-
 205 ics (e.g., see Visscher et al., 2010; Visscher & Moses, 2011, who estimated 420-2160 ppm

¹ For reference, a “protosolar” atmospheric water abundance is defined here as $X_{\text{H}_2\text{O}} = 830$ ppm or $X_{\text{H}_2\text{O}}/X_{\text{H}_2} = 9.61 \times 10^{-4}$ using elemental abundances from Lodders (2010) and accounting for the removal of some oxygen into rock (e.g., Visscher et al., 2010). For conversion between mole fraction abundances and element-to- H_2 mixing ratios on Jupiter, a hydrogen abundance of $X_{\text{H}_2} = 0.864$ is adopted based upon *Galileo* measurements of the He abundance (Niemann et al., 1998; von Zahn et al., 1998).

H₂O). More recently, Wang et al. (2015) showed that for a narrower range of rapid mixing rates expected near equatorial latitudes, the kinetic schemes of Visscher and Moses (2011) and Venot et al. (2012) give 85-640 ppm H₂O and 2500-9300 ppm H₂O, respectively. Full resolution of model differences (caused by differences in adopted rates of key reactions in the CO \rightleftharpoons CH₄ reaction scheme) may require improved understanding of the dynamical behavior of Jupiter's deep atmosphere and/or new studies that explore whether the reaction networks adapted from H-C-O combustion experiments under oxidizing conditions will behave consistently in hydrogen-rich planetary environments (e.g., see Moses et al., 2011; Venot et al., 2012, 2020; Moses, 2014; Wang et al., 2015, for further discussion). In the meantime, chemical models of the deep atmosphere will also be improved by new observational constraints on Jupiter's composition far below the clouds.

Looking Below the Clouds

The spatial distribution of cloud-forming species such as NH₃ and H₂O mapped by JIRAM provide information about the meteorological processes that affect their abundances in the cloud-forming region of Jupiter's troposphere ($\lesssim 10$ bar). For example, the observed H₂O relative humidity is highly variable with latitude (see Figure 2), with local enhancements in water vapor that appear to be associated with cyclonic regions consistent with models of moist convection (e.g., see Dowling & Gierasch, 1989; Roos-Serote et al., 2000; Ingersoll et al., 2004; Fletcher et al., 2017; Giles et al., 2015; Grassi et al., 2020). The distribution of NH₃ likewise shows abundance variations (see Figure 2) shaped by vertical and horizontal mixing, including an enhancement along the edges of the equatorial zone, a strong depletion near 10°N (consistent with microwave measurements; see Li et al., 2017, and discussion below), and longitudinal variations (including NH₃-rich plumes) near hot spot latitudes (e.g., see de Pater et al., 2016; Giles et al., 2017b; Li et al., 2017; Fletcher et al., 2016, 2020; Grassi et al., 2020).

While the JIRAM results provide new abundance estimates in the cloud-forming region of Jupiter's atmosphere, recent results from *Juno* Microwave Radiometer (MWR) measurements provide complementary estimates of the NH₃ and H₂O abundances well below the clouds (e.g., see Janssen et al., 2017). Because NH₃ absorbs more strongly than H₂O, MWR determinations of the water abundance require an accurate estimate of the NH₃ abundance profile, which is best constrained in the equatorial zone (e.g., Li et al., 2017). Using this approach (for 351 ppm NH₃ or 2.5 \times protosolar N), Li et al. (2020) obtain a deep H₂O abundance of 2500_{-1600}^{+2200} ppm (or $3.0_{-1.9}^{+2.6}$ \times protosolar H₂O) in the equatorial zone, confirming that the GPMS measurement (420 ppm) was not representative of Jupiter's deep water inventory. Combined with prior ground-based, spacecraft, and *in-situ* observations, the *Juno* results thus suggest roughly uniform (~ 2 - $4\times$) enhancements over protosolar abundances for several heavy elements in Jupiter's atmosphere.

The deep abundance measurements of the major cloud-forming species (Li et al., 2020) along with disequilibrium abundances (Grassi et al., 2020) can also be used to identify connections between the upper troposphere and the deep atmosphere, and to explore related questions about which chemical pathways, atmospheric motions, and meteorological processes are shaping the observed abundances of tropospheric chemical species: how deep does chemical variability extend? To what extent do deep atmospheric abundances represent bulk element inventories? For example, the MWR results show spatial variations in NH₃ extending to at least the ~ 50 bar level (e.g., see Li et al., 2017; Bolton et al., 2017; Ingersoll et al., 2017) with a deep abundance (~ 360 ppm) less than that observed by GPMS (570 ppm; Wong et al., 2004). In addition, high-resolution *Juno* measurements of Jupiter's gravity field suggest the presence of a diluted core and the possibility that the heavy element inventory is not uniformly mixed throughout the planet as a whole (e.g., see Wahl et al., 2017; Debras & Chabrier, 2019), presenting new challenges for inferring the chemical consequences of Jupiter's atmospheric evolution.

257 Nevertheless, the observed Jovian water inventory provides a key constraint on the
 258 composition of the material accreted, the timing and location of formation, and the in-
 259 ternal chemical and structural evolution of Jupiter over the history of the Solar System.
 260 A bulk oxygen inventory similar to that of other heavy elements (as suggested by *Juno*
 261 MWR results) calls into question formation scenarios that predict either very large or
 262 very small water abundances, whereas models that predict roughly similar heavy-element
 263 enhancements invite a closer look (e.g., see Owen et al., 1999; Lodders, 2004; Guillot &
 264 Hueso, 2006; Wong et al., 2008; Mousis et al., 2019, for references and further discus-
 265 sion). The new results also raise ongoing questions about core-accretion and gravitational
 266 collapse during giant planet formation: should we consider Jupiter to be uniformly *en-*
 267 *riched* in heavy elements? Or instead *depleted* in H and He? Our understanding of gi-
 268 ant planet formation within an evolving protoplanetary disk – informed by ongoing ground-
 269 based and *Juno* observations of key species in Jupiter’s troposphere – will continue shape
 270 how these questions are addressed both inside and outside of our own planetary system.

271 Acknowledgments

272 I thank the two anonymous reviewers for their reviews and many constructive sugges-
 273 tions that were incorporated into the commentary. No new data were generated in the
 274 preparation of this manuscript. Data used for the abundance profiles in Figure 2 are in-
 275 cluded in Grassi et al. (2020) and the full JIRAM datasets can be found in Grassi (2019).

276 References

- 277 Antuñano, A., Fletcher, L. N., Orton, G. S., Melin, H., Milan, S., Rogers, J., . . .
 278 Giles, R. (2019, September). Jupiter’s Atmospheric Variability from Long-term
 279 Ground-based Observations at 5 μm . *Astronomical Journal*, 158(3), 130. doi:
 280 10.3847/1538-3881/ab2cd6
- 281 Bézard, B., Lellouch, E., Strobel, D., Maillard, J.-P., & Drossart, P. (2002, Septem-
 282 ber). Carbon Monoxide on Jupiter: Evidence for Both Internal and External
 283 Sources. *Icarus*, 159(1), 95-111. doi: 10.1006/icar.2002.6917
- 284 Bjoraker, G. L., de Pater, I., Wong, M. H., Adamkovics, M., Hewagama, T., & Hes-
 285 man, B. (2016, October). Volatile Abundances and the Deep Cloud Structure
 286 in Jupiter’s Great Red Spot. In *Aas/division for planetary sciences meeting*
 287 *abstracts #48* (p. 508.05).
- 288 Bjoraker, G. L., Wong, M. H., de Pater, I., Hewagama, T., Ádámkovics, M., &
 289 Orton, G. S. (2018, September). The Gas Composition and Deep Cloud Struc-
 290 ture of Jupiter’s Great Red Spot. *Astronomical Journal*, 156(3), 101. doi:
 291 10.3847/1538-3881/aad186
- 292 Bolton, S. J., Adriani, A., Adumitroaie, V., Allison, M., Anderson, J., Atreya, S., . . .
 293 Wilson, R. (2017, May). Jupiter’s interior and deep atmosphere: The initial
 294 pole-to-pole passes with the *Juno* spacecraft. *Science*, 356(6340), 821-825. doi:
 295 10.1126/science.aal2108
- 296 Borunov, S., Dorofeeva, V., Khodakovsky, I., Drossart, P., Lellouch, E., & Encre-
 297 naz, T. (1995, February). Phosphorus chemistry in atmosphere of Jupiter: A
 298 reassessment. *Icarus*, 113, 460-464. doi: 10.1006/icar.1995.1036
- 299 D’Angelo, G., & Lissauer, J. J. (2018). Formation of Giant Planets. In *Handbook of*
 300 *exoplanets* (p. 140). doi: 10.1007/978-3-319-55333-7_140
- 301 de Pater, I., Sault, R. J., Butler, B., DeBoer, D., & Wong, M. H. (2016, June). Peer-
 302 ing through Jupiter’s clouds with radio spectral imaging. *Science*, 352(6290),
 303 1198-1201. doi: 10.1126/science.aaf2210
- 304 Debras, F., & Chabrier, G. (2019, February). New Models of Jupiter in the Context
 305 of *Juno* and *Galileo*. *Astrophysical Journal*, 872(1), 100. doi: 10.3847/1538
 306 -4357/aaff65
- 307 Dowling, T. E., & Gierasch, P. J. (1989, June). Cyclones and Moist Convection

- 308 on Jovian Planets. In *Bulletin of the American Astronomical Society* (Vol. 21,
309 p. 946).
- 310 Drossart, P., Lellouch, E., Bezdard, B., Maillard, J. P., & Tarrogo, G. (1990, Jan-
311 uary). Jupiter: Evidence for a Phosphine Enhancement at high Northern
312 latitudes. *Icarus*, *83*(1), 248-253. doi: 10.1016/0019-1035(90)90018-5
- 313 Fegley, B., Jr., & Lodders, K. (1994, July). Chemical models of the deep atmo-
314 spheres of Jupiter and Saturn. *Icarus*, *110*, 117-154. doi: 10.1006/icar.1994
315 .1111
- 316 Fegley, B., Jr., & Prinn, R. G. (1985, December). Equilibrium and nonequilib-
317 rium chemistry of Saturn's atmosphere - Implications for the observability
318 of PH₃, N₂, CO, and GeH₄. *Astrophysical Journal*, *299*, 1067-1078. doi:
319 10.1086/163775
- 320 Fegley, B., Jr., & Prinn, R. G. (1988, January). Chemical constraints on the water
321 and total oxygen abundances in the deep atmosphere of Jupiter. *Astrophysical*
322 *Journal*, *324*, 621-625. doi: 10.1086/165922
- 323 Flasar, F. M., & Gierasch, P. J. (1977). Eddy diffusivities within Jupiter. In
324 A. V. Jones (Ed.), *Planetary atmospheres* (p. 85). Ottawa: Royal Society of
325 Canada.
- 326 Fletcher, L. N. (2017, May). Cycles of activity in the Jovian atmosphere. *Geophysi-*
327 *cal Research Letters*, *44*(10), 4725-4729. doi: 10.1002/2017GL073806
- 328 Fletcher, L. N., Greathouse, T. K., Orton, G. S., Sinclair, J. A., Giles, R. S., Irwin,
329 P. G. J., & Encrenaz, T. (2016, November). Mid-infrared mapping of Jupiter's
330 temperatures, aerosol opacity and chemical distributions with IRTF/TEXES.
331 *Icarus*, *278*, 128-161. doi: 10.1016/j.icarus.2016.06.008
- 332 Fletcher, L. N., Orton, G. S., Greathouse, T. K., Rogers, J. H., Zhang, Z., Oya-
333 fuso, F. A., ... Adriani, A. (2020, March). Jupiter's Equatorial Plumes and
334 Hot Spots: Spectral Mapping from Gemini/TEXES and Juno/MWR. *arXiv*
335 *e-prints*, arXiv:2004.00072.
- 336 Fletcher, L. N., Orton, G. S., Rogers, J. H., Giles, R. S., Payne, A. V., Irwin,
337 P. G. J., & Vedovato, M. (2017, April). Moist convection and the 2010-
338 2011 revival of Jupiter's South Equatorial Belt. *Icarus*, *286*, 94-117. doi:
339 10.1016/j.icarus.2017.01.001
- 340 Fletcher, L. N., Orton, G. S., Teanby, N. A., & Irwin, P. G. J. (2009, August).
341 Phosphine on Jupiter and Saturn from Cassini/CIRS. *Icarus*, *202*(2), 543-564.
342 doi: 10.1016/j.icarus.2009.03.023
- 343 Giles, R. S., Fletcher, L. N., & Irwin, P. G. J. (2015, September). Cloud structure
344 and composition of Jupiter's troposphere from 5- μ m Cassini VIMS spec-
345 troscopy. *Icarus*, *257*, 457-470. doi: 10.1016/j.icarus.2015.05.030
- 346 Giles, R. S., Fletcher, L. N., & Irwin, P. G. J. (2017a, June). Latitudinal variability
347 in Jupiter's tropospheric disequilibrium species: GeH₄, AsH₃ and PH₃. *Icarus*,
348 *289*, 254-269. doi: 10.1016/j.icarus.2016.10.023
- 349 Giles, R. S., Fletcher, L. N., Irwin, P. G. J., Orton, G. S., & Sinclair, J. A. (2017b,
350 November). Ammonia in Jupiter's Troposphere From High-Resolution 5 μ m
351 Spectroscopy. *Geophysical Research Letters*, *44*(21), 10,838-10,844. doi:
352 10.1002/2017GL075221
- 353 Gomes, R., Levison, H. F., Tsiganis, K., & Morbidelli, A. (2005, May). Origin of
354 the cataclysmic Late Heavy Bombardment period of the terrestrial planets.
355 *Nature*, *435*(7041), 466-469. doi: 10.1038/nature03676
- 356 Grassi, D. (2019). Content of minor species in Jupiter's upper tropo-
357 sphere as inferred from Juno JIRAM data (PJ1-15). Mendeley Data, v1.
358 (<http://dx.doi.org/10.17632/cjs32jv68g.1>)
- 359 Grassi, D., Adriani, A., Mura, A., Atreya, S. K., Fletcher, L. N., Lunine, J. I., ...
360 Turrini, D. (2020, April). On the Spatial Distribution of Minor Species in
361 Jupiter's Troposphere as Inferred From Juno JIRAM Data. *Journal of Geo-*
362 *physical Research (Planets)*, *125*(4), e06206. doi: 10.1029/2019JE006206

- 363 Guillot, T., & Hueso, R. (2006, March). The composition of Jupiter: sign of a (rel-
 364 atively) late formation in a chemically evolved protosolar disc. *Monthly Notices*
 365 *of the Royal Astronomical Society*, *367*(1), L47-L51. doi: 10.1111/j.1745-3933
 366 .2006.00137.x
- 367 Helled, R., Bodenheimer, P., Podolak, M., Boley, A., Meru, F., Nayakshin,
 368 S., ... Boss, A. P. (2014, January). Giant Planet Formation, Evolu-
 369 tion, and Internal Structure. In H. Beuther, R. S. Klessen, C. P. Dulle-
 370 mond, & T. Henning (Eds.), *Protostars and Planets VI* (p. 643). doi:
 371 10.2458/azu_uapress.9780816531240-ch028
- 372 Ingersoll, A. P., Adumitroaie, V., Allison, M. D., Atreya, S., Bellotti, A. A., Bolton,
 373 S. J., ... Steffes, P. G. (2017, August). Implications of the ammonia
 374 distribution on Jupiter from 1 to 100 bars as measured by the Juno mi-
 375 crowave radiometer. *Geophysical Research Letters*, *44*(15), 7676-7685. doi:
 376 10.1002/2017GL074277
- 377 Ingersoll, A. P., Dowling, T. E., Gierasch, P. J., Orton, G. S., Read, P. L., Sánchez-
 378 Lavega, A., ... Vasavada, A. R. (2004). Dynamics of Jupiter's atmosphere.
 379 In F. Bagenal, T. E. Dowling, & W. B. McKinnon (Eds.), *Jupiter. The*
 380 *Planet, Satellites and Magnetosphere* (p. 105-128). Cambridge: Cambridge
 381 Univ. Press.
- 382 Irwin, P. G. J., Parrish, P., Fouchet, T., Calcutt, S. B., Taylor, F. W., Simon-
 383 Miller, A. A., & Nixon, C. A. (2004, November). Retrievals of jovian
 384 tropospheric phosphine from Cassini/CIRS. *Icarus*, *172*, 37-49. doi:
 385 10.1016/j.icarus.2003.09.027
- 386 Janssen, M. A., Oswald, J. E., Brown, S. T., Gulkis, S., Levin, S. M., Bolton, S. J.,
 387 ... Wang, C. C. (2017, November). MWR: Microwave Radiometer for the
 388 Juno Mission to Jupiter. *Space Science Reviews*, *213*(1-4), 139-185. doi:
 389 10.1007/s11214-017-0349-5
- 390 Kaye, J. A., & Strobel, D. F. (1983, June). HCN formation on Jupiter: The cou-
 391 pled photochemistry of ammonia and acetylene. *Icarus*, *54*(3), 417-433. doi: 10
 392 .1016/0019-1035(83)90238-5
- 393 Li, C., Ingersoll, A., Bolton, S., Levin, S., Janssen, M., Atreya, S., ... Zhang, Z.
 394 (2020). The water abundance in Jupiter's equatorial zone. *Nature Astron.* doi:
 395 10.1038/s41550-020-1009-3
- 396 Li, C., Ingersoll, A., Janssen, M., Levin, S., Bolton, S., Adumitroaie, V., ...
 397 Williamson, R. (2017, June). The distribution of ammonia on Jupiter from
 398 a preliminary inversion of Juno microwave radiometer data. *Geophysical Re-*
 399 *search Letters*, *44*(11), 5317-5325. doi: 10.1002/2017GL073159
- 400 Lodders, K. (2004, August). Jupiter formed with more tar than ice. *Astrophysical*
 401 *Journal*, *611*, 587-597. doi: 10.1086/421970
- 402 Lodders, K. (2010, January). Solar System Abundances of the Elements. *Astro-*
 403 *physics and Space Science Proceedings*, *16*, 379. doi: 10.1007/978-3-642-10352
 404 -0_8
- 405 Lunine, J. I., Coradini, A., Gautier, D., Owen, T. C., & Wuchterl, G. (2004). The
 406 origin of Jupiter. In F. Bagenal, T. E. Dowling, & W. B. McKinnon (Eds.),
 407 *Jupiter. The Planet, Satellites and Magnetosphere* (p. 19-34). Cambridge:
 408 Cambridge Univ. Press.
- 409 Mahaffy, P. R., Niemann, H. B., Alpert, A., Atreya, S. K., Demick, J., Donahue,
 410 T. M., ... Owen, T. C. (2000, June). Noble gas abundance and isotope ratios
 411 in the atmosphere of Jupiter from the *Galileo* Probe Mass Spectrometer. *Jour-*
 412 *nal of Geophysical Research*, *105*, 15061-15072. doi: 10.1029/1999JE001224
- 413 Morley, C. V., Skemer, A. J., Allers, K. N., Marley, M. S., Faherty, J. K., Visscher,
 414 C., ... Bjoraker, G. L. (2018, May). An L Band Spectrum of the Coldest
 415 Brown Dwarf. *Astrophysical Journal*, *858*, 97. doi: 10.3847/1538-4357/
 416 aabe8b
- 417 Moses, J. I. (2014, March). Chemical kinetics on extrasolar planets. *Philosophical*

- 418 *Transactions of the Royal Society of London Series A*, 372(2014), 20130073-
 419 20130073. doi: 10.1098/rsta.2013.0073
- 420 Moses, J. I., Visscher, C., Fortney, J. J., Showman, A. P., Lewis, N. K., Griffith,
 421 C. A., ... Freedman, R. S. (2011, August). Disequilibrium carbon, oxygen,
 422 and nitrogen chemistry in the atmospheres of HD 189733b and HD 209458b.
 423 *Astrophysical Journal*, 737, 15.
- 424 Mousis, O., Ronnet, T., & Lunine, J. I. (2019, April). Jupiter's Formation in the
 425 Vicinity of the Amorphous Ice Snowline. *Astrophysical Journal*, 875(1), 9. doi:
 426 10.3847/1538-4357/ab0a72
- 427 Niemann, H. B., Atreya, S. K., Carignan, G. R., Donahue, T. M., Haberman, J. A.,
 428 Harpold, D. N., ... Way, S. H. (1998, September). The composition of the
 429 Jovian atmosphere as determined by the *Galileo* probe mass spectrometer.
 430 *Journal of Geophysical Research*, 103, 22831-22846. doi: 10.1029/98JE01050
- 431 Orton, G. S., Fisher, B. M., Baines, K. H., Stewart, S. T., Friedson, A. J., Ortiz,
 432 J. L., ... Parija, K. C. (1998, September). Characteristics of the Galileo
 433 probe entry site from Earth-based remote sensing observations. *Journal of*
 434 *Geophysical Research*, 103, 22791-22814. doi: 10.1029/98JE02380
- 435 Owen, T., Mahaffy, P., Niemann, H. B., Atreya, S., Donahue, T., Bar-Nun, A., & de
 436 Pater, I. (1999, November). A low-temperature origin for the planetesimals
 437 that formed Jupiter. *Nature*, 402, 269-270.
- 438 Prinn, R. G., & Barshay, S. S. (1977, December). Carbon monoxide on Jupiter and
 439 implications for atmospheric convection. *Science*, 198, 1031-1034.
- 440 Raymond, S. N., Izidoro, A., & Morbidelli, A. (2018, December). Solar Sys-
 441 tem Formation in the Context of Extra-Solar Planets. *arXiv e-prints*,
 442 arXiv:1812.01033.
- 443 Roos-Serote, M., Vasavada, A. R., Kamp, L., Drossart, P., Irwin, P., Nixon, C., &
 444 Carlson, R. W. (2000, May). Proximate humid and dry regions in Jupiter's
 445 atmosphere indicate complex local meteorology. *Nature*, 405(6783), 158-160.
 446 doi: 10.1038/35012023
- 447 Strobel, D. F. (1977, June). NH₃ and PH₃ photochemistry in the Jovian atmo-
 448 sphere. *Astrophysical Journal Letters*, 214, L97-L99. doi: 10.1086/182450
- 449 Taylor, F. W., Atreya, S. K., Encrenaz, T., Hunten, D. M., Irwin, P. G. J., & Owen,
 450 T. C. (2004). The composition of the atmosphere of Jupiter. In F. Bagenal,
 451 T. E. Dowling, & W. B. McKinnon (Eds.), *Jupiter. The Planet, Satellites and*
 452 *Magnetosphere* (p. 59-78). Cambridge: Cambridge Univ. Press.
- 453 Tsiganis, K., Gomes, R., Morbidelli, A., & Levison, H. F. (2005, May). Origin
 454 of the orbital architecture of the giant planets of the Solar System. *Nature*,
 455 435(7041), 459-461. doi: 10.1038/nature03539
- 456 Venot, O., Cavalié, T., Bounaceur, R., Tremblin, P., Brouillard, L., & Lhous-
 457 saine Ben Brahim, R. (2020, February). New chemical scheme for gi-
 458 ant planet thermochemistry. Update of the methanol chemistry and new
 459 reduced chemical scheme. *Astronomy & Astrophysics*, 634, A78. doi:
 460 10.1051/0004-6361/201936697
- 461 Venot, O., Hébrard, E., Agúndez, M., Dobrijevic, M., Selsis, F., Hersant, F., ...
 462 Bounaceur, R. (2012, October). A chemical model for the atmosphere of hot
 463 Jupiters. *Astronomy & Astrophysics*, 546, A43. doi: 10.1051/0004-6361/
 464 201219310
- 465 Visscher, C., Lodders, K., & Fegley, B., Jr. (2006, September). Atmospheric Chem-
 466 istry in Giant Planets, Brown Dwarfs, and Low-Mass Dwarf Stars. II. Sulfur
 467 and Phosphorus. *Astrophysical Journal*, 648, 1181-1195. doi: 10.1086/506245
- 468 Visscher, C., & Moses, J. I. (2011, September). Quenching of Carbon Monoxide and
 469 Methane in the Atmospheres of Cool Brown Dwarfs and Hot Jupiters. *Astro-*
 470 *physical Journal*, 738(1), 72. doi: 10.1088/0004-637X/738/1/72
- 471 Visscher, C., Moses, J. I., & Saslow, S. A. (2010, October). The deep water abun-
 472 dance on Jupiter: New constraints from thermochemical kinetics and diffusion

- 473 modeling. *Icarus*, 209(2), 602-615. doi: 10.1016/j.icarus.2010.03.029
474 von Zahn, U., Hunten, D. M., & Lehmacher, G. (1998, September). Helium in
475 Jupiter's atmosphere: Results from the *Galileo* probe helium interferome-
476 ter experiment. *Journal of Geophysical Research*, 103, 22815-22830. doi:
477 10.1029/98JE00695
- 478 Wahl, S. M., Hubbard, W. B., Militzer, B., Guillot, T., Miguel, Y., Movshovitz, N.,
479 ... Bolton, S. J. (2017, May). Comparing Jupiter interior structure models to
480 Juno gravity measurements and the role of a dilute core. *Geophysical Research*
481 *Letters*, 44(10), 4649-4659. doi: 10.1002/2017GL073160
- 482 Wang, D., Gierasch, P. J., Lunine, J. I., & Mousis, O. (2015, April). New insights on
483 Jupiter's deep water abundance from disequilibrium species. *Icarus*, 250, 154-
484 164. doi: 10.1016/j.icarus.2014.11.026
- 485 Wang, D., Lunine, J. I., & Mousis, O. (2016, September). Modeling the disequilib-
486 rium species for Jupiter and Saturn: Implications for Juno and Saturn entry
487 probe. *Icarus*, 276, 21-38. doi: 10.1016/j.icarus.2016.04.027
- 488 Wong, M. H., Lunine, J. I., Atreya, S. K., Johnson, T., Mahaffy, P. R., Owen, T. C.,
489 & Encrenaz, T. (2008, January). Oxygen and Other Volatiles in the Giant
490 Planets and their Satellites. *Reviews in Mineralogy and Geochemistry*, 68(1),
491 219-246. doi: 10.2138/rmg.2008.68.10
- 492 Wong, M. H., Mahaffy, P. R., Atreya, S. K., Niemann, H. B., & Owen, T. C. (2004,
493 September). Updated *Galileo* probe mass spectrometer measurements of car-
494 bon, oxygen, nitrogen, and sulfur on Jupiter. *Icarus*, 171, 153-170. doi: 10
495 .1016/j.icarus.2004.04.010